Solar Phys (2009) 260: 451–463
DOI 10.1007/s11207-009-9446-2

Study of Distribution and Asymmetry of Solar Active Prominences during Solar Cycle 23

Navin Chandra Joshi · Neeraj Singh Bankoti · Seema Pande · Bimal Pande · Kavita Pandey

Received: 9 September 2008 / Accepted: 24 August 2009 / Published online: 2 October 2009

Abstract In this article we present the results of a study of the spatial distribution and asymmetry of solar active prominences (SAP) for the period 1996 through 2007 (solar cycle 23). For more meaningful statistical analysis we analyzed the distribution and asymmetry of SAP in two subdivisions *viz*. Group1 (ADF, APR, DSF, CRN, CAP) and Group2 (AFS, ASR, BSD, BSL, DSD, SPY, LPS). The North – South (N – S) latitudinal distribution shows that the SAP events are most prolific in the 21° to 30° slice in the Northern and Southern Hemispheres; the East – West (E – W) longitudinal distribution study shows that the SAP events are most prolific (best observable) in the 81° to 90° slice in the Eastern and Western Hemispheres. It was found that the SAP activity during this cycle is low compared to previous solar cycles. The present study indicates that during the rising phase of the cycle the number of SAP events are roughly equal in the Northern and Southern Hemispheres. However, activity in the Southern Hemisphere has been dominant since 1999. Our statistical study shows that the N – S asymmetry is more significant then the E – W asymmetry.

Keywords Sun: activity · Sun: prominences · Sun: North – South and East – West asymmetry

1. Introduction

Long-term observations of various solar activity phenomena indicate that their occurrence in the Northern and Southern (as well as Eastern and Western) Hemispheres on the solar disk are not uniform, with more events occurring in one or the other hemisphere during certain periods of time. This phenomenon is referred to as asymmetry. The North – South (N – S) and East – West (E – W) distribution and asymmetries of several solar activity phenomena, such as flares, filaments, magnetic flux, relative sunspot numbers, coronal mass ejections (CMEs), and sunspot areas were investigated by various authors (Maunder, 1904; Howard, 1974; Knoška, 1985; Verma, 1987; Vizoso and Ballester, 1987; Verma, 1993;

N.C. Joshi (✉) · N.S. Bankoti · S. Pande · B. Pande · K. Pandey
Department of Physics, DSB Campus, Kumaun University, Naini Tal 263 002, Uttarakhand, India
e-mail: njoshi98@gmail.com

Oliver and Ballester, 1994; Verma, 2000a; Verma, 2000b; Temmer *et al.*, 2001; Joshi and Pant, 2005; Gao, Li, and Zhong, 2007). Much work was done to study the distribution and asymmetry since Maunder (1904) observed and presented the N – S asymmetry of sunspots during the period 1874 – 1902. Verma (2000b) investigated the N – S and E – W distribution and asymmetries of the solar active prominences (SAP) events for the whole disk for the period 1957 to 1998 in considerable detail. Many authors paid particular attention to the asymmetry of the photospheric features (sunspot relative number, sunspot area, magnetic classes of sunspots, etc.) and their relation to the phase of the 11-year solar cycle (SC). Vizoso and Ballester (1987) presented the results of a study of the N – S asymmetry in sudden disappearances of solar prominences (SDP) during solar cycles 18 through 21. The asymmetries of all solar active features in the entire solar atmosphere were also studied. Verma (1987) studied the N – S asymmetry for major flares, Type II radio bursts, white-light flares, gamma-ray bursts, and hard X-ray bursts. Brajša *et al.* (2005) analyzed spatial distribution and N – S asymmetry of coronal bright points from mid-1998 to mid-1999.

Some of the authors (Carbonell, Oliver, and Ballester, 1993; Li, Schmieder, and Li, 1998; Ataç and Özgüç, 2001) demonstrated that the N – S asymmetry has high statistical significance. The E – W asymmetry of solar phenomena also was studied by various authors (Letfus, 1960; Letfus and Růžičková-Topolová, 1980; Joshi, 1995) and the existence of a small asymmetry was reported. This means that the non-uniformity of the solar activity (N – S asymmetry in particular) is a real feature and therefore cannot be due to random fluctuations generated from a binomial or uniform distribution of probability between hemispheres. Other authors tried to find a periodicity in this distribution. First, an 11 to 12 year periodicity was inferred, but whether or not it is related to the classical sunspot cycle is still controversial. Nevertheless, most of them found that the asymmetry is not in phase with the 11-year SC (Garcia, 1990; Vizoso and Ballester, 1990; Temmer *et al.*, 2001). Long-term periods were also suggested: 8 SCs (Vizoso and Ballester, 1990; Ataç and Özgüç, 1996) and even 12 SCs (Verma, 1992; Li *et al.*, 2002). Based on such studies the asymmetry of the solar activity in SC 23 should favor the Southern Hemisphere.

In the present article we investigate the spatial distribution and asymmetry of SAP for the period 1996 through 2007 (SC 23). In Section 2 we present the observational data and analysis. In Section 3 the latitudinal distributions and N – S asymmetry are discussed. In Section 4 we discuss the longitudinal distributions and E – W asymmetry. Our approach consists of examining the ascending, maximum, and descending phase of SC 23. In Section 5 we present the comparison between SC 20, 21, 22, and 23, and in the final section, Section 6, results and discussions are presented.

2. Observation Data and Analysis

The data used in the present study were collected from National Geophysical Data Center's (NGDC's) anonymous ftp server from 1 January 1996 to 31 December 2007. This period covers SC 23. The URL address of this website is as follows: ftp://ftp.ngdc.noaa.gov/STP/SOLAR_DATA/SOLAR_FILAMENTS. The SAP data include limb and disk features and events. During this period of 4383 days, the occurrence of a total number of 8778 SAP are reported. From this database the events that occurred at 0^{o} latitude and central meridian distance (CMD) were excluded. After excluding such events, we get a total of 8732 SAP for the N – S distribution and 8712 SAP for the E – W distribution. Table 1 lists different limb and disk features and their corresponding percentages.

From this table we can see that the disappearing filament (DSF) is the most dominating feature, whereas DSF, arch filament system (AFS), dark surge on disk (DSD), and active

Table 1 The number of different limb and disk features and the corresponding percentage values during SC 23.

Limb and disk features		Group number	Number of events	%
DSF	(Disappearing filament)	1	1962	22.35
AFS	(Arch filament system)	2	1923	21.91
DSD	(Dark surge on disc)	2	1488	16.95
ADF	(Active dark filament)	1	1202	13.69
BSL	(Bright surge on limb)	2	600	6.84
ASR	(Active surge region)	2	574	6.54
APR	(Active prominence)	1	344	3.92
EPL	(Eruptive prominence on limb)		336	3.83
LPS	(Loops)	2	155	1.77
BSD	(Bright surge on disc)	2	146	1.66
SPY	(Spray)	2	33	0.38
CAP	(Cap prominence)	1	14	0.16
CRN	(Coronal rain)	1	1	0.01
SSB	(Solar sector boundary)		0	0.00
MDP	(Mound prominence)		0	0.00
Total			8778	100.00

Table 2 Number of events in the two subgroups and the corresponding percentage values during SC 23.

Group	Number	%
G1: ADF, APR, DSF, CRN, CAP	3523	41.73
G2: AFS, ASR, BSD, BSL, DSD, SPY, LPS	4919	58.27
Total	8442	100.00

dark filament (ADF) together give 74.90% of the total SAP events during the period of study for SC 23. For a more meaningful statistical analysis we analyzed different features separately along with the total SAP data. For this we formed two groups related as far as physics is concerned: Group 1 (G1), for structures belonging to prominence/filament and Group 2 (G2), those belonging to active regions. The eruptive prominence on limb (EPL) data were left out because EPL is an ambiguous group that contains eruptions of prominences as well as solar flare eruptions close to the limb and thus cannot be distributed equally among the two subgroups chosen. Table 2 lists the number of features in two subgroups and their percentage values. It shows that G2 consists of a larger number of features (58.27%) compared to G1 (41.73%). The yearly variation of different features during the SC 23 can be clearly seen from Table 7.

In Figure 1, the monthly number of SAP, monthly number of G1 and G2, and monthly mean sunspot number (SN) during the period of our investigation are plotted. This figure also represents the plots for the monthly number of Hα solar flares and subflares (SF) as well as for the solar flare index (Q) therein. We included all Hα flare events having importance equal to and greater than subflare. The flare index (Q) represents daily flare activity observed during a 24 h period. It is calculated for each flare using the formula $Q = i \times t$, where i is the importance coefficient of the flare and t is the

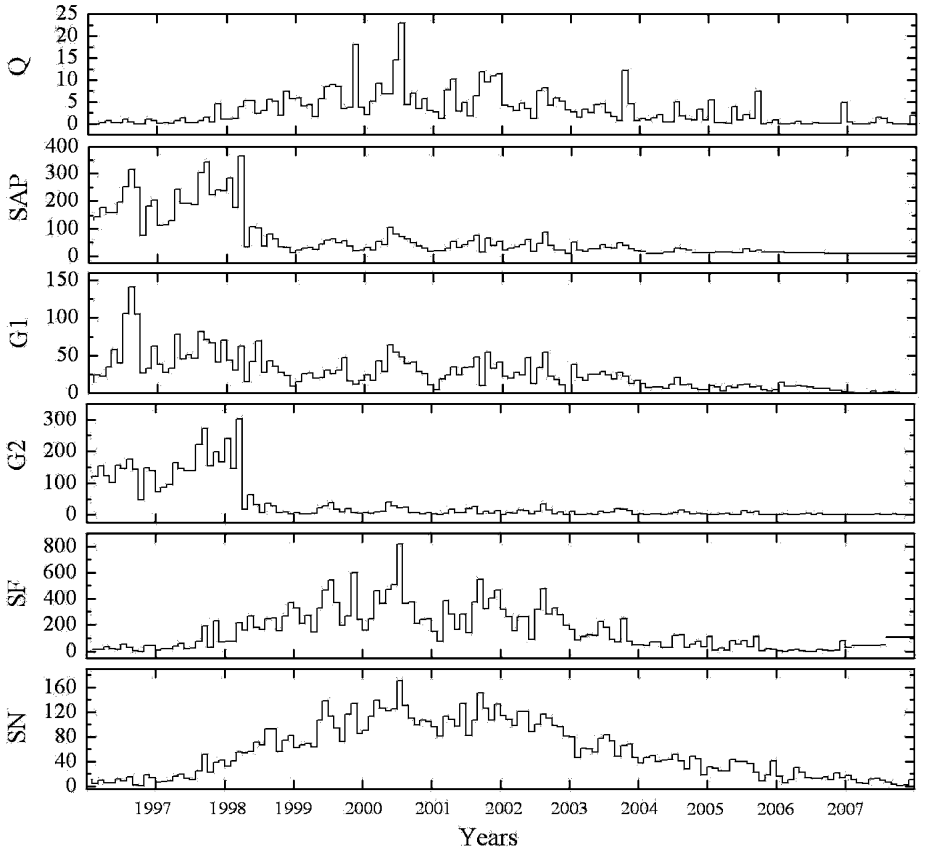

Figure 1 Monthly plots of different solar activity parameters, flare index (Q), solar active prominences (SAP), Group1 (G1), Group2 (G2), Hα solar flares and subflares (SF), and sunspot number (SN) from 1996 – 2007 (from top to bottom panel).

duration of the flare in minutes (Kleczek, 1952). SF, SN data, and the calculated values of Q are available in anonymous ftp servers of NGDC. The addresses of these websites are as follows: ftp://ftp.ngdc.noaa.gov/STP/SOLAR_DATA/SOLAR_FLARES/INDEX and ftp://ftp.ngdc.noaa.gov/STP/SOLAR_DATA/SUNSPOT_NUMBERS.

From Figure 1 we can see that the variation of Q, SF, and SN is similar, but different from the SAP and both G1 and G2. During the ascending phase of SC 23, SAP, G1, and G2 are maximum in number, but other phenomena, i.e., SF and SN are minimum in number. However, after 1999 this contrasting appearance (in SAP, SF, and SN) is not exhibited. From the year 1996 and beyond 1998, G1 shows similar variation to SAP, while G2 all along shows a similar behavior to that of SAP, barring the peak height before 1997. Figure 1 shows peaks during the maximum phase (2000 – 2001) of the SC under investigation.

2.1. Statistical Analysis

To specify the statistical significance of the N – S and E – W asymmetry indices, we followed Letfus (1960) and Letfus and Růžičková-Topolová (1980). We calculated the N – S

asymmetry indices (A_{NS}) and E – W asymmetry indices (A_{EW}) using the formula

$$A_{NS} = \frac{N - S}{N + S}, \qquad A_{EW} = \frac{E - W}{E + W}. \tag{1}$$

The dispersion of the N – S and E – W asymmetry of a random distribution of flares is given by

$$\Delta A_{NS} = \pm \frac{1}{\sqrt{2(N + S)}}, \tag{2}$$

$$\Delta A_{EW} = \pm \frac{1}{\sqrt{2(E + W)}}. \tag{3}$$

Here N and S are the numbers of SAP observed in the northern and southern halves of the solar disk and E and W are the number of SAP observed in the eastern and western halves, respectively. Thus, if $A_{NS} > 0$, the activity in the northern hemisphere dominates, if not it will dominate the southern hemisphere. Similarly, if $A_{EW} > 0$, the activity in the eastern hemisphere dominates, otherwise it will dominate the western hemisphere.

To verify the reliability of the observed N – S and E – W asymmetry values a χ^2-test is applied using Equations (4) and (5), given below, respectively.

$$\chi_{NS} = \frac{2(N + S)}{\sqrt{(N + S)}} = \frac{\sqrt{2}A_{NS}}{\Delta A_{NS}}, \tag{4}$$

$$\chi_{EW} = \frac{2(E + W)}{\sqrt{(E + W)}} = \frac{\sqrt{2}A_{EW}}{\Delta A_{EW}}. \tag{5}$$

If $A_{NS} = \Delta A_{NS}$ and $A_{EW} = \Delta A_{EW}$, the probability that the asymmetry exceeds the dispersion value is $p = 84\%$, and if $A_{NS} = 2\Delta A_{NS}$ and $A_{EW} = 2\Delta A_{EW}$ p is 99.5%. Here the first limit differentiates between the statistically significant and insignificant values and the second separates the values that may be considered quite realistic. The limits divide the values of the asymmetry into three categories: with low probabilities, intermediate probabilities, and high probabilities (Joshi, 1995; Temmer *et al.*, 2001; Joshi and Joshi, 2004).

3. Latitudinal Distribution and N – S Asymmetry

The SAP data obtained from NGDC were analyzed to understand the N – S distribution and N – S asymmetry. In Table 3 we show the yearly number of SAP events at an interval of 10° in the Northern and Southern Hemispheres. Column 12 of Table 3 gives the total number of SAP in the Northern and Southern Hemispheres. In Figure 2(a), we plot the number of SAP, G1, and G2 *versus* heliographic latitude in degrees for SC 23. The 0° latitude represents the equator of the Sun. From Figure 2(a) it is clear that the SAP as well as G1 and G2 activity is at maximum between 21° and 30° latitude in each hemisphere. The N – S asymmetry indices based on the annual counts from 1996 to 2007 for SAP, G1, and G2 are plotted in Figure 2(b). From this figure it is clear that all curves show similar behavior. In 1997 the cycle was Northern Hemisphere dominated, but after 1999 it becomes Southern Hemisphere dominant and stays there for the remaining years. Out of 12 N – S asymmetry values eight turn out to be highly significant with a probability $p \geq 99.5\%$,

Table 3 Number of SAP in different latitude bands on the Northern (N) and Southern (S) Hemispheres and tabulated for each year. The dominant hemisphere (DH) and asymmetry index (A-Index) are given for all the years as well as for all the latitudinal bands. SAP that occurred at the equator are excluded.

Years		Number of SAP									Total	A-Index	DH
		1 – 10°	11 – 20°	21 – 30°	31 – 40°	41 – 50°	51 – 60°	61 – 70°	71 – 80°	81 – 90°			
1996	N	611	194	91	41	31	15	11	8	12	1014	−0.08360	S
	S	653	323	110	40	25	11	9	16	12	1199		
1997	N	194	398	657	173	27	6	2	0	4	1461	+0.16787	N
	S	92	178	581	151	32	3	0	3	1	1041		
1998	N	12	157	231	44	11	3	1	0	1	460	−0.30250	S
	S	12	230	427	119	50	17	0	2	2	859		
1999	N	15	61	72	40	19	8	6	1	1	223	+0.00677	N
	S	19	72	55	35	19	14	6	0	0	220		
2000	N	39	94	95	25	23	9	1	0	1	287	−0.02547	S
	S	48	106	78	39	20	10	1	0	0	302		
2001	N	35	64	63	37	13	1	0	0	0	213	−0.10879	S
	S	50	81	70	35	20	7	0	1	1	265		
2002	N	41	61	34	22	11	4	0	0	0	173	−0.15610	S
	S	38	86	65	28	14	5	0	1	0	237		
2003	N	55	37	28	28	9	2	1	0	0	160	−0.13747	S
	S	64	79	39	18	6	3	0	0	2	211		
2004	N	30	22	13	4	0	1	0	0	0	70	−0.14634	S
	S	38	36	10	4	1	3	0	0	2	94		
2005	N	20	28	5	3	3	0	0	0	2	61	−0.04688	S
	S	20	26	8	2	3	2	3	0	3	67		
2006	N	11	5	8	1	3	2	0	0	1	31	−0.39216	S
	S	17	16	14	17	4	2	0	0	1	71		
2007	N	3	2	0	0	0	0	0	0	0	5	−0.23077	S
	S	5	0	1	0	0	0	0	0	2	8		
Total	N	1066	1123	1297	418	150	51	22	9	22	4158	−0.04764	S
	S	1056	1233	1458	488	194	77	19	23	26	4574		
A-Index		+0.0047	−0.0467	−0.0584	−0.0772	−0.1280	−0.2031	+0.0732	−0.4375	−0.0833	−0.0476		
DH		N	S	S	S	S	S	N	S	S	S		

where the observed asymmetry index exceeds the dispersion value of a random distribution. Out of 12 values one and three come out to be statistically significant and insignificant, respectively. The highly significant, significant, and insignificant values of N – S asymmetry indices are marked with black squares, black stars, and white circles, respectively, in Figure 2(b).

4. Longitudinal Distribution and E – W Asymmetry

The data downloaded from NGDC were also used to study the E – W distribution of SAP, as well as G1 and G2, data for the period 1996 through 2007. In Table 4 we show the yearly

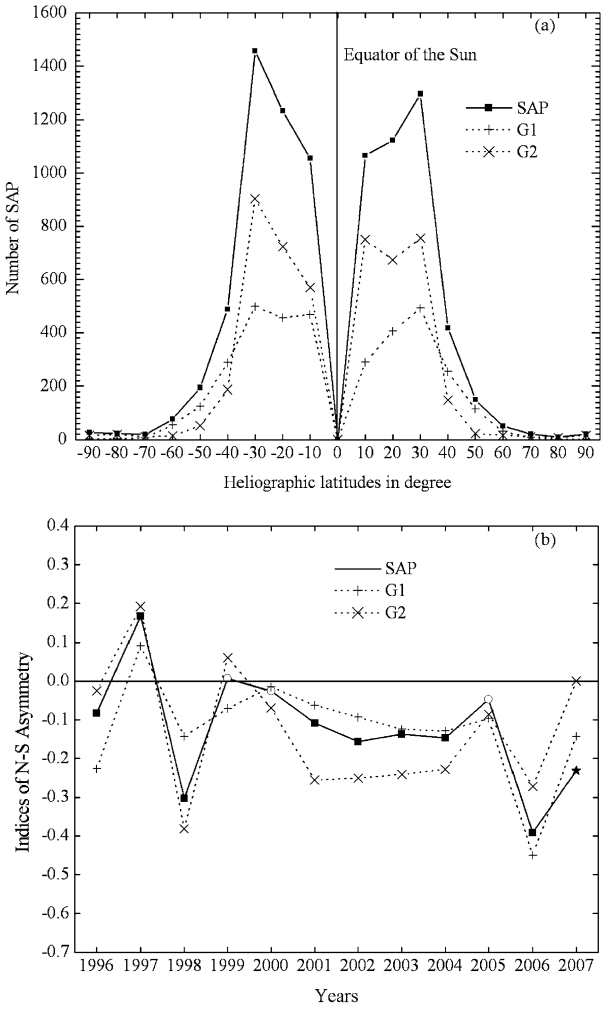

Figure 2 (a) Plot of the number of SAP (solid line), G1 and G2 (doted lines) *versus* North – South heliographic latitudes in degrees. (b). Plot of N – S asymmetry indices for SAP (solid line), G1 and G2 (doted lines) events *versus* years (1996 – 2007). Highly significant, significant, and insignificant values are marked with black squares (■), black stars (★), and white circles (○), respectively.

distribution of SAP events at central meridian distance (CMD) intervals of 10° from the central meridian toward the east and west limbs, respectively, during SC 23. To visualize the table, we plot the number of SAP, G1, and G2 *versus* heliographic CMD in degrees in Figure 3(a). In Figure 3(a) the minus (−) sign in heliographic CMD indicates Eastward and the plus (+) sign represents Westward, *e.g.*, −90° represents E90 and +90° represents W90. From Figure 3(a), it is clear that the number of SAP as well as G1 and G2 events decreases from 1° to 80° and then SAP, G1, and G2 frequency increase between 81° and 90° CMD. The E – W asymmetry indices for all SAP and the two subgroups (G1 and G2) *versus* year are plotted in Figure 3(b). From this figure it can be seen that all curves show the same type of behavior; five out of 12 asymmetry values reveal a high statistical significance with $p \geq 99.5\%$, while four and three of them come out to be significant and statistically insignificant, respectively. The highly significant, significant, and insignificant values of the E – W asymmetry indices are marked with black squares, black stars, and white circles, respectively, in Figure 3(b).

Table 4 Number of SAP at different CMD bands in the Eastern (E) and Western (W) Hemispheres and tabulated for each year. The dominant hemisphere (DH) and asymmetry index (A-Index) are given for all the years as well as for all the CMD bands. SAP that occurred at the central meridian are excluded.

Years		Number of SAP									Total	A-Index	DH
		1 – 10°	11 – 20°	21 – 30°	31 – 40°	41 – 50°	51 – 60°	61 – 70°	71 – 80°	81 – 90°			
1996	E	172	133	140	132	94	56	48	26	178	979	−0.11643	W
	W	206	170	163	133	119	86	75	28	257	1237		
1997	E	189	195	207	162	148	125	84	40	140	1290	+0.03907	E
	W	157	180	177	152	129	108	54	35	201	1193		
1998	E	93	90	74	67	68	50	40	13	120	615	−0.06606	W
	W	73	102	76	65	72	53	34	21	206	702		
1999	E	22	21	25	24	16	11	12	11	83	225	+0.01351	E
	W	19	30	17	17	15	19	12	4	86	219		
2000	E	33	45	27	30	18	17	8	6	90	274	−0.06644	W
	W	42	34	21	39	23	31	5	7	111	313		
2001	E	38	50	19	34	18	10	11	4	66	250	+0.04384	E
	W	39	26	30	31	18	9	6	3	67	229		
2002	E	17	15	25	17	19	13	7	2	59	174	−0.14914	W
	W	28	25	18	30	20	9	5	3	97	235		
2003	E	24	18	20	19	14	17	13	2	50	177	−0.04065	W
	W	24	32	21	18	21	15	10	2	49	192		
2004	E	7	9	16	18	5	3	3	2	18	81	−0.01220	W
	W	10	8	11	6	11	6	2	1	28	83		
2005	E	7	8	6	5	7	2	4	4	17	60	−0.07692	W
	W	8	14	6	7	0	5	2	2	26	70		
2006	E	11	8	3	5	5	7	1	1	12	53	+0.03922	E
	W	9	9	11	8	1	1	1	0	9	49		
2007	E	1	1	0	0	0	0	0	0	2	4	−0.33333	W
	W	3	2	0	0	1	1	1	0	0	8		
Total	E	614	593	562	513	412	311	231	111	835	4182	−0.03994	W
	W	618	632	551	506	430	343	207	106	1137	4530		
A-Index		−0.0033	−0.0318	+0.0099	+0.0069	−0.0214	−0.0490	+0.0548	+0.0230	−0.1531	−0.03994		
DH		W	W	E	E	W	W	E	E	W	W		

5. Comparison among Solar Cycles 20, 21, 22, and 23

Verma (2000b) calculated the yearly number of the SAP events in 10° latitude bands for the Northern and Southern Hemispheres as well as for the Eastern and Western Hemispheres, respectively, from 1957 to 1998. In Tables 5 and 6 of our article, we count and present the total number of SAP events for SCs 20, 21, 22, and 23 in the interval of 10° latitude and CMD from 0° to 90°. We consider the data from 1963 to 2007 covering the four SCs. The N – S and E – W asymmetry of SAP events is shown by the solid lines in Figures 4 and 5, with highly significant, significant, and insignificant values marked with black squares, black stars, and white circles, respectively. Thirty-seven out of 45 N – S asymmetry values reveal a high statistical significance with $p \geq 99.5\%$. Of these, one and seven come out to be statistically significant and insignificant, respectively. Out of 45 E – W asymmetry values,

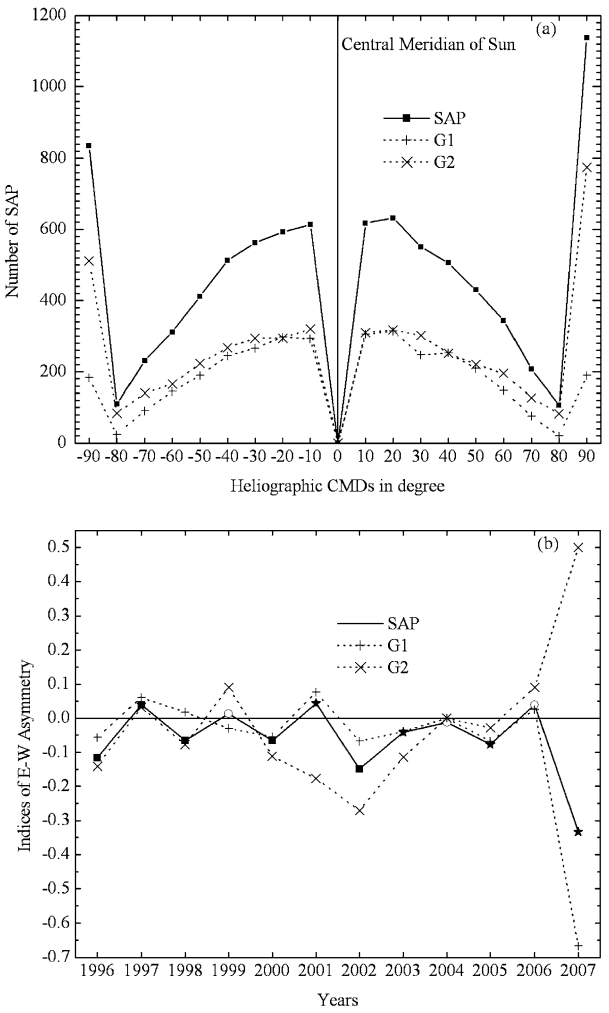

Figure 3 Same as Figure 2, but for CMDs distribution and E – W asymmetry.

29 reveal a high statistical significance with $p \geq 99.5\%$, whereas ten and six out of 45 turn out to be significant and statistically insignificant, respectively. In Figure 4, we also plot the N – S asymmetry in the sudden disappearances of solar prominences (SDP) for the period 1947 to 1985 (Vizoso and Ballester, 1987) by the dotted line.

6. Discussions and Conclusions

In the present study the distribution of SAP, G1, and G2 in the Northern and Southern (as well as Eastern and Western) Hemispheres for SC 23 are analyzed. The results obtained are as follows:

- From the equator of the Sun the frequency of SAP, G1, and G2 events increases from 1° to 30° and then decreases from 31° to 90°. The SAP events are at maximum between latitudes 21° to 30° for SC 23, but for the SCs 20, 21, and 22 SAP activity are at maximum between the 11° to 20° latitude band on either side of the solar equator.

Table 5 Total number of SAP at different latitude bands in the northern (N) and southern (S) hemispheres and tabulated for four SCs. The dominant hemisphere (DH) and asymmetry index (A-Index) are given for four solar cycles. SAP that occurred exactly at the equator are excluded.

Cycle		Total number of SAP									Total	A-Index	DH
		1 – 10°	11 – 20°	21 – 30°	31 – 40°	41 – 50°	51 – 60°	61 – 70°	71 – 80°	81 – 90°			
20	N	6039	10922	7533	2285	713	325	220	145	113	28295	+0.22487	N
	S	5621	7175	3355	886	383	251	98	69	68	17906		
21	N	2553	3141	1585	759	350	210	247	281	297	9423	+0.00943	N
	S	2343	3193	1757	648	351	228	214	259	254	9247		
22	N	10400	12505	7064	2646	760	370	333	311	373	34762	−0.05233	S
	S	9246	16034	8555	2875	798	347	240	237	269	38601		
23	N	1066	1123	1297	418	150	51	22	9	22	4158	−0.04764	S
	S	1056	1233	1458	488	195	76	19	23	26	4574		

Table 6 Number of SAP at different CMD bands in the eastern (E) and western (W) hemispheres and tabulated for four SCs. The dominant hemisphere (DH) and asymmetry index (A-Index) are given for four solar cycles. SAP that occurred exactly at the central meridian are excluded.

Cycle		Total number of SAP									Total	A-Index	DH
		1 – 10°	11 – 20°	21 – 30°	31 – 40°	41 – 50°	51 – 60°	61 – 70°	71 – 80°	81 – 90°			
20	E	1948	1807	1705	1487	1222	863	593	502	13191	23318	+0.00955	E
	W	1839	1640	1654	1409	1187	815	566	510	13257	22877		
21	E	558	590	496	480	355	318	196	91	6535	9619	+0.03037	E
	W	572	526	530	515	377	311	190	103	5928	9052		
22	E	4453	4452	4289	4078	3783	3241	2546	1647	10049	38538	−0.03966	W
	W	5074	4804	4612	4307	3873	3471	2562	1820	11198	41721		
23	E	614	593	562	513	412	311	231	111	835	4182	−0.03994	W
	W	618	632	551	506	430	343	207	106	1137	4530		

- From the central meridian of the Sun, the frequency of SAP, G1, and G2 events decreases from 1° to 80° and the frequency increases between 81° to 90°. The SAP events are most numerous between the 81° to 90° CMD band.
- From Tables 5 and 6 it is found that the SAP activity during this cycle is low compared to the previous four SCs.
- From the statistical analysis it is clear that N – S asymmetry is more significant than the E – W asymmetry.

Comparing latitudinal distribution during SC 23 [Figure 2(a)] with four previous SCs (see Figure 3 in Verma, 2000b) it can be seen that SAP events are most prolific in 21° through 30°. This is different from the previous SCs (11 – 20°), whereas the CMD distribution [Figure 3(a)] shows similar behavior (see Figure 1 in Verma, 2000b). For SC 23 the SAP events are not uniformly distributed in the Northern and Southern Hemispheres. The southern dominance of solar activity during SC 23 was investigated by several authors using different solar activity features, i.e., solar flares and CMEs (Joshi, Pant, and Manoharan, 2006; Gao, Li, and Zhong, 2007). Similar trends are found in the present investigation with SAP data. The present study and the study of Ataç and Özgüç (1996) confirm the predictions of Verma (1992) for SC 23. According to Verma (1992) the N – S asymmetry of solar active

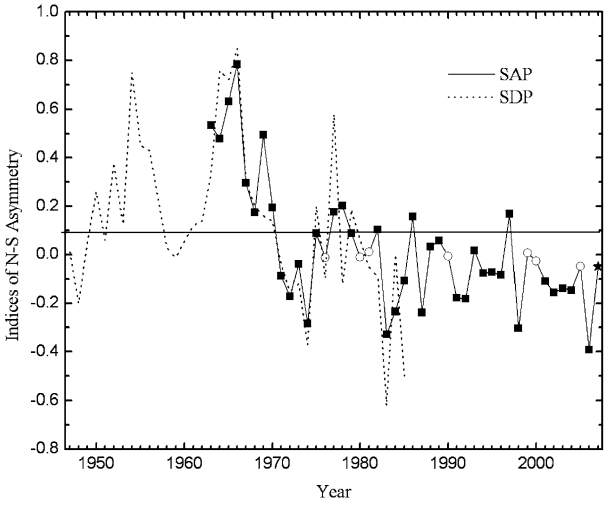

Figure 4 Plot of the N – S asymmetry indices of SAP events *versus* years (1963 – 2007). Highly significant, significant, and insignificant values are marked with black squares (■), black stars (★), and white circles (○), respectively.

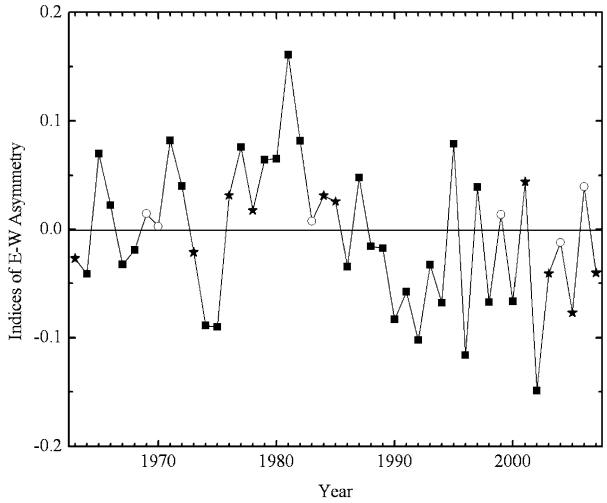

Figure 5 Same as Figure 4 but for E – W asymmetry.

phenomena would be southern dominated during SCs 22, 23, and 24 and will be northern dominated during SC 25. Temmer *et al.* (2001) presented a statistical analysis of Hα flares from 1975 to 1999 and found that there exists a significant N – S asymmetry and slight, but significant, E – W asymmetry. Similar results are also found in our study.

Tables 3 and 4 show many interesting aspects of SAP distribution (latitude and CMD) with the evolution of SC 23. From Table 3 it is clear that, in the ascending phase of the cycle, the number of SAP first increases from 1996 to 1997 and then decreases from 1998 to the end of the cycle under investigation. In 1996 the highest number of SAP events were observed in the $\pm 10°$ latitude belt. Durung the years after 1996, most of the SAP are located in the 21° to 30° latitude belt; with the progress of the cycle the number of SAP decreased while the maximum numbers shifted to lower latitudes. Table 4 shows that at the beginning of the cycle the frequency of SAP peaked both in low (1 – 10°) as well as in high (81 – 90°) CMD bands. In 1997, just after the solar minimum, most SAP events were located between

Table 7 Number of SAP (limb and disk features) tabulated for each year.

Years	Number of SAP (limb and disk features)															Total
	DSF	AFS	DSD	ADF	BSL	ASR	APR	EPL	LPS	BSD	SPY	CAP	CRN	SSB	MPD	
1996	107	635	528	490	184	194	61	9	2	27	0	1	0	0	0	2238
1997	112	931	572	464	13	258	67	12	2	74	1	0	0	0	0	2506
1998	237	353	242	117	91	93	34	76	29	41	2	5	0	0	0	1320
1999	204	1	31	30	76	10	35	42	10	0	4	3	0	0	0	446
2000	318	0	27	37	72	9	52	39	28	0	8	2	1	0	0	593
2001	296	0	19	18	41	6	39	24	28	3	5	0	0	0	0	479
2002	207	0	23	24	58	3	37	45	11	0	1	3	0	0	0	412
2003	247	0	18	8	35	0	4	34	22	0	4	0	0	0	0	372
2004	92	1	16	6	15	0	3	20	6	0	6	0	0	0	0	165
2005	65	0	7	4	10	1	6	22	15	1	1	0	0	0	0	132
2006	70	0	5	4	5	0	6	11	0	0	1	0	0	0	0	102
2007	7	2	0	0	0	0	0	2	2	0	0	0	0	0	0	13
Total	1962	1923	1488	1202	600	574	344	336	155	146	33	14	1	0	0	8778

21° and 30° and 81° and 90° CMD bands. It is clear from Tables 5 and 6 that indices of N – S and E – W asymmetry of SAP events favor the Northern and Western Hemisphere for SCs 20 and 21, and shift to the Southern and Eastern Hemisphere during cycles 22 and 23. Table 7 represents the yearly variation of different features of SAP during SC 23. It is clear from this table that most of the SAP events (69.08%) occur during the rising phase (1996, 1997, and 1998) of the cycle under investigation. From all SAP events AFS, DSD, ADF, bright surge on limb (BSL), active surge region (ASR), active prominence (APR), and bright surge on disk (BSD) reach maximum in number during the rising phase and decrease as the cycle progresses; whereas DSF, EPL, loops (LPS), and spray (SPY) are rare during the rising phase and reach a maximum during the maximum phase of the cycle. Comparing our results with that of Verma (2000b) we find that the variation of the N – S asymmetry index during SC 23 differs from that of the previous three cycles (*i.e.*, SCs 20, 21, and 22). From Figures 4 and 5 it is clear that the N – S and E – W asymmetry do not show any systematic behavior and have no relation with SCs maxima and minima during the last four solar cycles.

Acknowledgements The authors thank UGC, New Delhi for financial assistance under DSA (phase-III) program running in the Department of Physics, Kumaun University, Nainital. Two of the authors, NCJ and NSB, are thankful to UGC, New Delhi for financial assistance under RFSMS (Research Fellowship in Science for meritorious students) scheme. The authors are also thankful to the referee and editor for their valuable comments and suggestions.

References

Ataç, T., Özgüç, A.: 1996, *Solar Phys.* **166**, 201.
Ataç, T., Özgüç, A.: 2001, *Solar Phys.* **198**, 399.
Brajša, R., Wöhl, H., Vršnak, B., Ruždjak, V., Clette, F., Hochedez, J.-F., Verbanac, G., Temmer, M.: 2005, *Solar Phys.* **231**, 29.
Carbonell, M., Oliver, R., Ballester, J.L.: 1993, *Astron. Astrophys.* **274**, 497.
Garcia, H.A.: 1990, *Solar Phys.* **127**, 185.
Gao, P.X., Li, Q.X., Zhong, S.H.: 2007, *J. Astrophys. Astron.* **28**, 207.
Howard, R.: 1974, *Solar Phys.* **38**, 59.

Joshi, A.: 1995, *Solar Phys.* **157**, 315.
Joshi, B., Joshi, A.: 2004, *Solar Phys.* **219**, 343.
Joshi, B., Pant, P.: 2005, *Astron. Astrophys.* **431**, 359.
Joshi, B., Pant, P., Manoharan, P.K.: 2006, *J. Astrophys. Astron.* **27**, 151.
Kleczek, J.: 1952, *Publ. Czechoslov. Centr. Astron. Inst.* **22**.
Knoška, Š.: 1985, *Contrib. Astron. Obs. Skaln. Pleso* **13**, 217.
Letfus, V.: 1960, *Bull. Astron. Inst. Czechoslov.* **11**, 31.
Letfus, V., Růžičková-Topolová, B.: 1980, *Bull. Astron. Inst. Czechoslov.* **31**, 232.
Li, K.-J., Schmieder, B., Li, Q.-Sh.: 1998, *Astron. Astrophys. Suppl. Ser.* **131**, 99.
Li, J.K., Wang, J.X., Xiong, S.Y., Liang, H.F., Yun, H.S., Gu, X.M.: 2002, *Astron. Astrophys.* **383**, 648.
Maunder, E.W.: 1904, *Mon. Not. R. Astron. Soc.* **64**, 747.
Oliver, R., Ballester, J.L.: 1994, *Solar Phys.* **152**, 481.
Temmer, M., Veronig, A., Hanslmeier, A., Otruba, W., Messerotti, M.: 2001, *Astron. Astrophys.* **375**, 1049.
Verma, V.K.: 1987, *Solar Phys.* **114**, 185.
Verma, V.K.: 1992, *Astron. Soc. Pac. Conf. Ser.* **27**, 429.
Verma, V.K.: 1993, *Astrophys. J.* **403**, 797.
Verma, V.K.: 2000a, *J. Astrophys. Astron.* **21**, 173.
Verma, V.K.: 2000b, *Solar Phys.* **194**, 87.
Vizoso, G., Ballester, J.L.: 1987, *Solar Phys.* **112**, 317.
Vizoso, G., Ballester, J.L.: 1990, *Astron. Astrophys.* **229**, 540.